CARMEN: A Cellular Automaton Rain Flow Model with Evaporation and Infiltration

Thibault Desjonquères, Paulina Essunger, Hannes Nilsson, and Erik Norlin
Chalmers University of Technology

(Turtles Collaboration)
(Dated: January 7, 2023)

We have developed a cellular automaton model for the flow of rain water to investigate the impact of land use on the flow dynamics. The model includes surface flow, infiltration into the soil, and evaporation. The modeled region is the Oued Boukhalef basin in Morocco. We first model the basic water flow, starting with a 10 cm thick layer of water all over the region, and letting the water flow according to the rules for the cell updates. This simulation achieves surface water results that match a satellite image of the region. Next, we simulate the flow for four days, in real time. During the first two days, we let it rain intensely, after which the land is left to dry. We compare the flow dynamics for a theoretical fully urbanized land surface with that for the real land use of the considered region. Results show that for the considered weather conditions, an additional one-third the amount of water remains on the surface of the theoretical urbanized land, compared to the actual land use, which is mainly dedicated to agriculture. This highlights the importance of taking water management into account in the context of land-use policy decisions.

Keywords: Cellular automaton, Modeling, Simulations, Precipitation, Climate, Surface flow, Flooding, Land use

I. INTRODUCTION

Several kinds of extreme weather, such as heatwaves, droughts, and floods, are expected to increase in frequency and/or intensity with continued anthropogenic climate change [1]. Because a warmer atmosphere can hold more moisture, extreme precipitation events are also expected to increase in both intensity and frequency, and this has already been observed at the global level and in most regions [1]. Indeed, even though dry regions are expected to get drier, extreme precipitation is expected to increase there, too [2]. When an extreme rain event does occur, its impact will greatly depend on what happens to the water once it reaches the ground, which in turn depends on the intensity and duration of the event but also on the specific land conditions: the topography, land use, surface type, including soil type if applicable, as well as climate-related factors such as soil moisture and snow melt [3]. Certain combinations of these conditions can lead to flooding.

Higher average temperatures and changing weather patterns can increase the risk of flooding in various ways. For example, higher sea levels caused by thermal expansion and ice melt increase the risk of *coastal* flooding. *Pluvial* flooding, i.e., flooding related to precipitation, occurs when the precipitation intensity is greater than the drainage capacity. Pluvial flooding is a major source of the damage that extreme precipitation can cause [3]. Many different factors can contribute to pluvial flooding. For example, a normal precipitation event can lead to local flooding if a drainage system is clogged.

Drainage capacity depends on human-made and natural factors. The former include how the land is used (e.g., forestry, agriculture, urban development), construction of impermeable surfaces such as pavement and roofs; and the dimensions and maintenance of drainage systems, etc. Natural factors include topography, which directs flows; vegetation, which intercepts precipitation; and soil type, which helps determine the rate and amount of infiltration. Climate also impacts drainage capacity. Soil moisture, in particular, modulates the risk of flooding: drying soil conditions can reduce the risk [4]. Temperature affects evaporation, increasing atmospheric water vapor in the first place but also decreasing soil moisture. Attribution studies show that certain flooding events have been made more intense by precipitation that has in turn been made more extreme by climate change (cf. [5, 6]).

For traditional agricultural economies, periodic flooding can be beneficial or even necessary, especially in otherwise dry climates, by providing farmed flood plains with moisture and nutrients [7]. But as societies shift away from agriculture, land surfaces grow less permeable (just picture paving over a pasture). Understanding how rain water flows across these surfaces, infiltrates them, and evaporates from them and from the soil becomes all the more relevant.

This study constructs a cellular automaton model to simulate run-off, infiltration, and evaporation of rain to help understand how water moves across the land surface, see Fig. 1. This can aid in predicting flood risks, managing water resources, and designing infrastructure, such as storm water drainage systems and flood control, and also support decisions about land use. Our objective is to answer the following questions:

1. Can the water dynamics in a region in the real world be captured by a cellular automaton model?
2. How may the land use impact the risk of severe flooding?

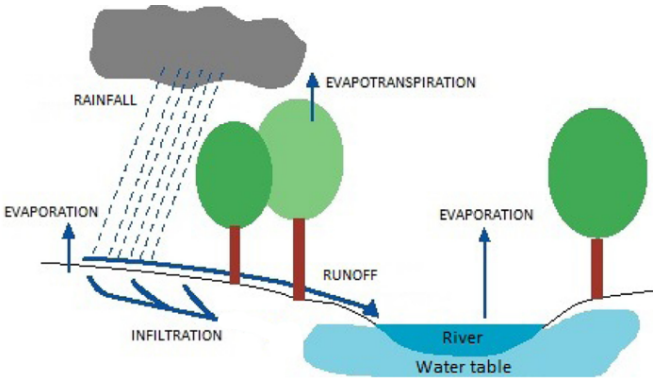

FIG. 1: Summary of the key elements of the water flow model. Adapted from [8].

II. THEORETICAL FRAMEWORK

We construct a cellular automaton to perform hydrological modeling. This section explains the two concepts.

A. Hydrological modeling

Hydrological modeling is way of characterizing the evolution of real hydrologic systems, such as water storage and water flux at the Earth's surface and subsurface, using mathematical analogies and computer simulations [9], [10]. Hydrological modeling is primarly used in water resources planning and management to gain insight about flood forecasting and climate impact assessments [11].

Hydrological simulations are often performed with Digital Elevation Models (DEM) where elevation data in a region is divided into cells, where the water flow direction from a given cell is the direction of steepest descent to an immediate neighbour [12].

B. Cellular automaton

A cellular automaton (CA) is a network of cells that change states depending on the states of their neighbours. The state of a cell is determined by a simple set of rules (every cell is governed by the same set of rules), which can allow for complex emergent behaviour at the global scale [13]. For modeling purposes, a CA can be interpreted as an idealized version of some physical system, discretized in time and space.

III. METHOD

To simulate water flow in a region, we implement a mathematical model inspired by the one in [8], which considers the Oued Boukhalef basin, west of Tangier in northern Morocco. A CA is used to update the water flow dynamics at two scales, i.e. water flow dynamics at the surface and into the soil. Kassogué et al. base their CA on a hexagonal grid, where each cell has six adjacent neighbors affecting its update rule. In our model, we use a square grid, and the set of neighboring cells is taken as the von Neumann neighborhood, consisting of the four closest neighbors only, located to the left, right, up and down respectively.

The update rules for the surface water flow and the infiltrated water are shown in equations 1 and 2, respectively, with the variables explained in Tables I and II.

$$Q_{ps}^{t+1} = Q_{ps}^{t} + Q_{r}^{[t]} - Q_{i}^{[t]} - Q_{vs}^{[t]} - Q_{e}^{[t]} \tag{1}$$

$$Q_{pi}^{t+1} = Q_{pi}^{t} + Q_{i}^{[t]} - Q_{vi}^{[t]} \tag{2}$$

TABLE I: Water quantities of cell $c_{i,j}$ measured at time step t in m^3.

Symbol	Explanation
$Q_{pi}^{t}(i,j)$	Quantity of water in the soil
$Q_{ps}^{t}(i,j)$	Quantity of water on the surface

TABLE II: Dynamic flow quantities for cell $c_{i,j}$ measured between time steps t and $t+1$ in m^3.

Symbol	Explanation
$Q_{e}^{[t]}(i,j)$	Quantity of drained water
$Q_{i}^{[t]}(i,j)$	Quantity of infiltrated water
$Q_{r}^{[t]}(i,j)$	Quantity of received water
$Q_{vs}^{[t]}(i,j)$	Quantity of water evaporated from the surface
$Q_{vi}^{[t]}(i,j)$	Quantity of water evaporated from the soil

We spare the readers the rather involved calculations of the dynamic flow quantities. For the full details, see [8]. Minor differences arise from the fact that our model is based on a square grid. Since we consider the von Neumann neighborhood, the difference is that all neighbors have the same distance to the center cell in our case, which simplifies the calculations a bit. In order to visualize the evolution of the water into the land, the cells are categorized by four states, depending on the level of saturation of the soil and the amount of surface water, see Section V. Results.

IV. IMPLEMENTATION

As detailed below, we implement our model in Python, using elevation and land-use data for the basin, to run two experiments to investigate our research questions. See Fig. 2 for a summary of our implementation.

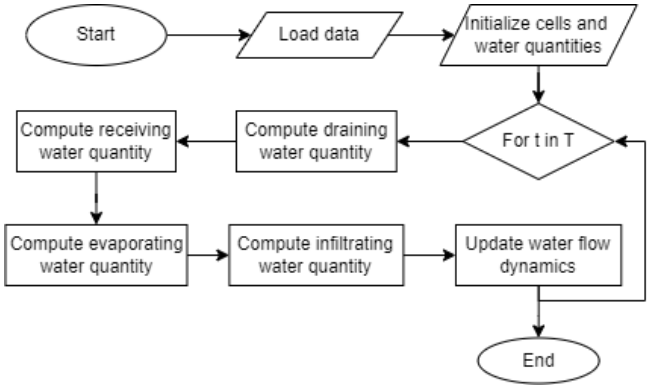

FIG. 2: Flowchart of the implemented model. First, elevation and land use data are loaded from csv files. Second, cells are initialized and assigned properties based on the data and a chosen water level. Then, as the model runs, in each time step, every type of water quantity is computed for each cell and the dynamics are updated based on these quantities.

A. Data

Elevation and land-use data for the region were gathered from the authors of the paper to simulate the water flow over the land (see Fig. 3). A CA was used to model water flow over the region where each data point represented cells on a grid and each cell corresponded to a two-dimensional piece of 25-by-25 meters of squarely shaped land of the particular area being modeled. More precisely, the region was divided into a 338-by-328 grid of cells, each cell holding the relevant information about the land in the specific corresponding parts of the region. Such features include static land-specific properties, such as the elevation, and features of the ground. These properties affect the amount of water a cell can hold and the rate of flow between cells in the grid, and are fed to the update rules of the corresponding cell at any time step.

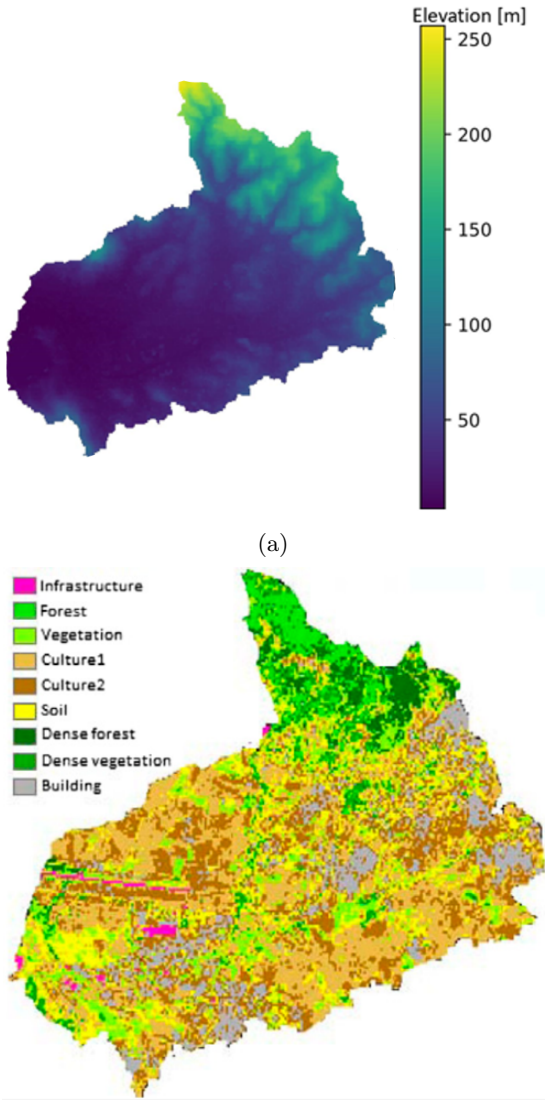

FIG. 3: (a) Elevation and (b) land-use data for Oued Boukhalef basin in Morocco. The northeast part of the region is mountainous, with forest in the far northern protrusion. Data shared by Kassagoue et al. via private communication; the land-use data (b) is Fig. 8.d in [8]).

B. Object oriented programming (OOP)

Considering the large number of properties to keep track of for all cells simultaneously, the implementation of the model is done using object-oriented programming, with all code written in Python. Each cell is created as an instance of a customized object, and all cell instances are linked to each other by assigning them pointers to the corresponding neighboring cells to form the structure of the physical region. In addition, the cell object is constructed with all the properties a cell must hold, with functions to update them for new conditions to study, or as the simulation progresses. The cell objects are stored in a 2D array encapsulating the region, making it easy to reference each cell by index and visualize the region as a whole. Since the region is not squarely shaped, and no data exist for the land outside, the indices corresponding to positions outside the region are simply left empty.

C. Flow dynamics

Apart from land-specific properties, each cell was linked to a set of water quantities, distinguishing water present on the surface from water absorbed by the ground. These quantities are fed to the update rules, and the different types affect the water flow differently. We used the standard CA format of a single universal update rule, independent of the position of the cells and the particular time. The water quantities are the focus, and they are what the updating rules govern, so that they alone constitute the dynamics. All other parameters are held constant over each run. Various scenarios were modeled by changing the initial conditions. More precisely, to investigate the two research questions, we designed two experiments.

D. Experiment I: Capturing the true water flow dynamics of the region.

As an initial experiment, we aimed at reconstructing natural waterways in the region. This investigation would provide insight into the ability of the model to capture the true water flow dynamics. We first initialized each cell with 10 cm of surface water and let the model flow for 24 hours. Iterating the dynamics lets the cells redistribute the water through drainage, infiltration and evaporation, according to their update rules.

E. Experiment II: Studying the effects of land use on flooding during heavy rainfall.

In the second part of the study, starting with no water on the surface, nor in the soil, 8 mm of rain was added each hour for 48 hours straight. This corresponds to very heavy rain, as defined in [14]. The rainfall was followed by an additional 48 hours of clear weather to conclude the simulation. First, we ran the simulation considering the land use as given in the actual data from the region. As can be seen in Fig. 3(b), the majority of the land corresponds to agricultural areas in this case, with a fair amount of forest, and some urbanized regions. We monitored the quantities of water present on the surface and in the soil, during and after the heavy rainfall. To study the effect of changes in land use on the risk of flooding, an identical setup as in the first simulation was constructed, apart from the land use. Instead of storing the actual land-use data in each respective cell, we initiated them with parameters corresponding to infrastructure. This changed the properties of the individual cells, allowing us to study the global changes in the dynamics. A realistic analogy of this would be for the city of Tangier to expand, with the agricultural areas and forest reserves covered by asphalt, concrete, and buildings.

V. RESULTS

We briefly present the results from our two experiments.

A. Experiment I: Capturing the water flow dynamics of the region.

Fig. 4(a) shows the surface water at the final stage of the simulation for Experiment I, aiming at verifying that the modeled water flow is physically correct. Infiltration and evaporation are included. The simulated flow is compared with the actual river system shown in the satellite image of region in Fig. 4(b).

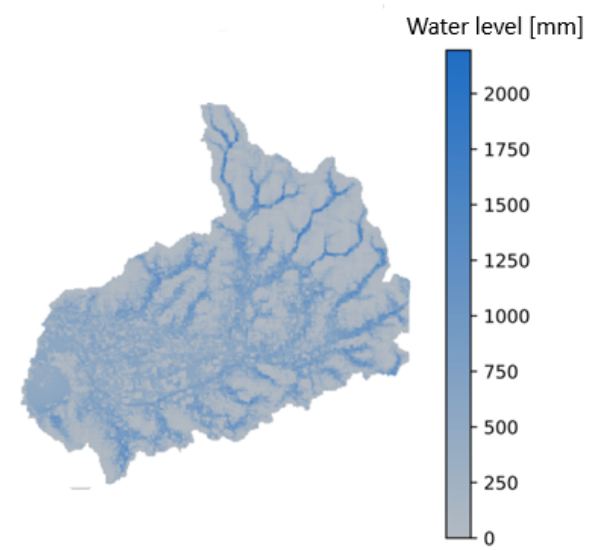

(a)

(b)

FIG. 4: (a) Simulated water flow in experiment I, where water is uniformly initialized on the land and left to flow, infiltrate, evaporate. (One-day simulation). (b) Actual satellite image of river system (Figure 10(b) in Kassogué et al. [8]). Note how the simulation (a) approximately recovers the waterways seen in the satellite image (b).

B. Experiment II: Studying the effects of land use on flooding during heavy rainfall.

Figs. 5a and 5c represent the distribution of the surface water at the end of the rain-and-dry simulation, using (a) the actual land surface and (c) a theoretical, fully urbanized land. An additional one-third the amount of water remains at the surface of the theoretical all-urbanized land, compared to the actual land, see Figs. 5b and 5d, which show the total surface and infiltrated water throughout the simulation for the two land-use cases.

The states of the land at key stages of the simulation for the second experiment are represented in Fig. 6.

VI. DISCUSSION

The water flow, including infiltration and evaporation shown in Fig. 4 appears to concur with the actual river system observed from the satellite image of the considered land in Fig. 4(b). Though, one could question why the water of the river system from the experiment doesn't resemble the water of the satellite image exactly. The purpose of this experiment was to test that the water dynamics worked; that water would end up in the contours of the river system that the satellite image shows, but not necessarily match it precisely. Since we artificially initialized an arbitrary quantity of water evenly across the entire region, which isn't a realistic scenario, it makes sense that the result does not match the satellite image precisely.

From this point, the land use can be modified in order to investigate different flow dynamics.

By generating maps of the state of the cell, we observe that the urbanized areas get saturated first at the beginning of the simulation, as shown in Fig. 6(a). Shortly after, water remains detained at the surface across most of the land due to surface water detention, as shown in Fig. 6(b). This surface water then infiltrates the soil, saturating all the agricultural areas. The forest areas remain unsaturated at this stage, as shown in Fig. 6(c). At the moment when the rain stops, 384 mm of water has fallen onto the land. Soon after the rain has stopped, the entire land has become saturated, and only evaporation takes place, desaturating the land progressively in Fig. 6(d). Fig. 6(e) shows the effects of the evaporation on the land at the end of the simulation.

Figs. 5a and 5c indicate that much more water persists at the surface of the urbanized land than on the land with a lot of agriculture. Additional expansion of the city of Tangier would therefore require additional water management efforts. Figs. 5b and 5d illustrate how the presence of forests and agriculture impacts the dynamics of the water, as they allow about a fourth of the surface water to infiltrate the soil, reducing the amount of surface water considerably. Also, the presence of forests and agriculture increases the rate of evaporation over the land. This is due to their higher crop factor K_c in the Blaney-Criddle formula, described in further detail in [8]. In Fig. 5b, the initially high rate of infiltration decreases first when the agriculture lands saturate, and then again when the forests have saturated, at a much later time.

A. Grid structure

One difference in our model compared to the one by [15] is that we use a square lattice version, considering von Neumann neighborhoods. In their CA, a hexagonal structure was employed. As per [16], both versions come with a set of pros and cons. The main source of criticism toward the square structure is a problem commonly referred to as *the island effect*. The underlying issue here is that squarely distributed cells have close-by neighbors with infinitely narrow borders at the corners. The hexagonal structure is argued to better represent the flowing phenomena since it effectively restructures the area to eliminate these oblique border cases. On the downside, though, this restructuring adds additional operations, since the standard form of the collected input data comes in squarely distributed data. Furthermore, the visualization tools used to display the results of the simulation takes in image type data in square or rectangular format. In other words, these conversions add additional computational complexity, and it is argued that the advantages are not worth the overhead. Therefore, the square format remains the standard for grid-based hydrological modeling.

This dispute among scientists makes the comparison between our model, and the one by [15] particularly interesting. Although this study covers other objectives, and so also has other differences in the setup compared to ours than just the structure of the grid, the simulations do correspond to similar enough settings to provide some insight into the global differences. Although not clear from the presented plots alone, it appears when comparing the reconstruction the rivers that form in the northeast region of the model, and stretches out toward the southwest, that the water flows faster in their model. One possible explanation for this behavior comes from the island effect. As previously discussed, the infinitely narrow boarders do raise concerns about the accuracy of the flow dynamics. In reality, if the largest height difference between certain regions is in the diagonal direction, most of the water would likely flow in that direction naturally. In our model, however, the water is forced to take a longer path in a zigg-zagg pattern of alternating downward and leftward steps. One way to deal with this is to instead use hexagonal structure. Another alternative would be to instead of von Neumann neighborhoods consider Moore neighborhoods. This would take the additional four diagonal neighbors of a cell into account, albeit with a difference weight corresponding to their relatively large distance to the center cell, as discussed by Argun et al. in [17]. In retrospect, we may have wanted

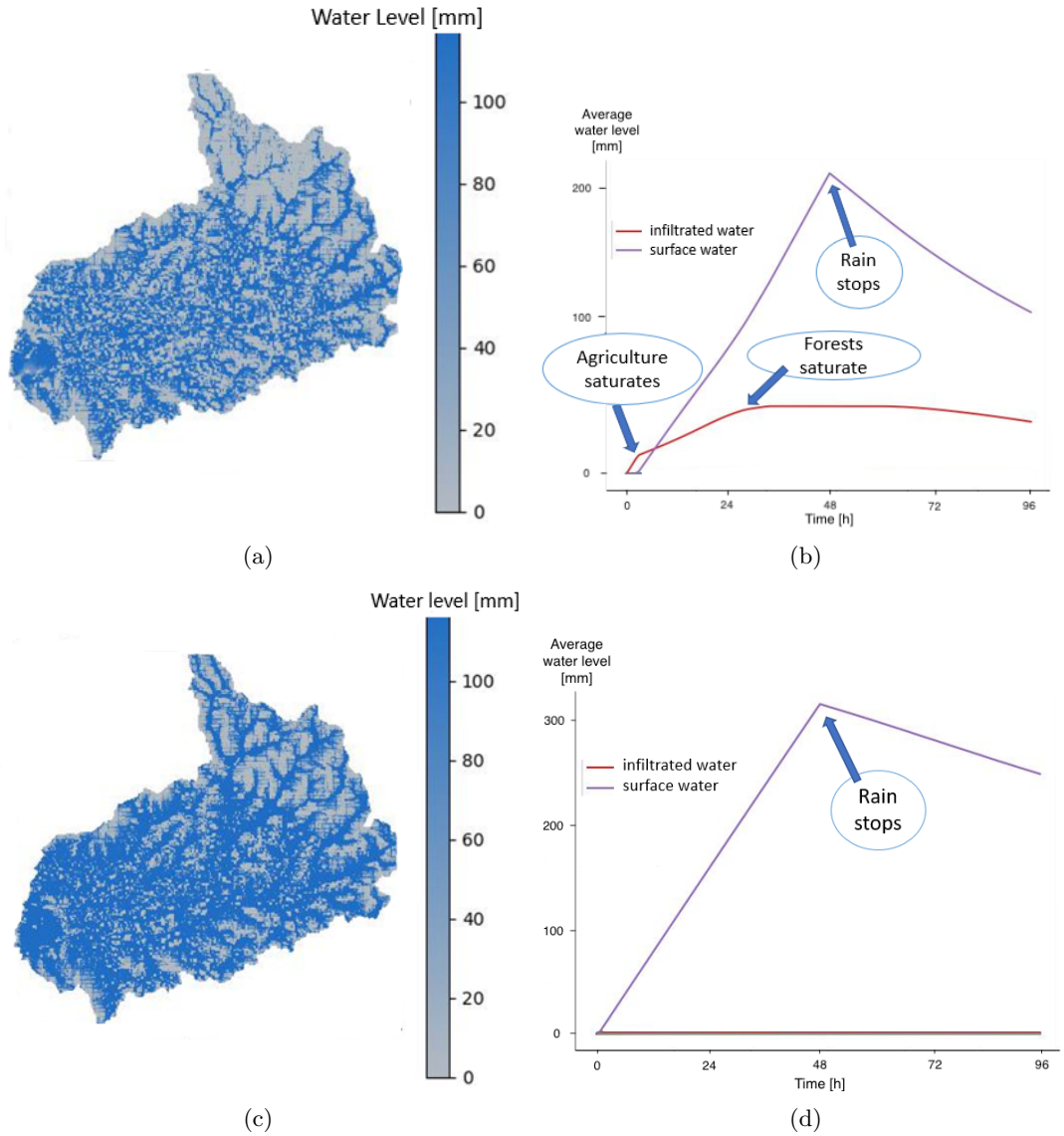

FIG. 5: Results from simulation with 48h of heavy rain (8mm/h), followed by 48h of clear weather, in the cases of actual land use, and hypothetical fully urbanized land. (a) Distribution of water on the surface in the studied region at the end of the simulation considering actual land use. (b) Amount of surface and infiltrated water for an average cell in the region during the simulation considering actual land use. (c) Distribution of water on the surface in the studied region at the end of the simulation considering fully urbanized land. (d) Amount of surface and infiltrated water for an average cell in the region during the simulation considering fully urbanized land. Note how changing the land use to infrastructure leads to a significant increase in the average surface water level.

to consider a differently structured cellular automaton.

B. Approximation of parameters

The infiltration capacity, initially a soil type property, has been mapped to a land use property, as soil type data was not accessible for this study. This approximation made sense because land use and soil type are correlated, for example, the soil type of land use infrastructure are more likely to consist of cement and asphalt, hence, having a lower infiltration capacity.

Since the infiltration and surface water detention is not realistically accurate set in this study the results becomes more demonstrative of what one can do with the model rather than realistic results to rely on for future work.

The temperature of the region which was used to simulate evaporation was set to the constant average temperature over a year which could effect the results greatly. Some months have lower temperature and therefore less

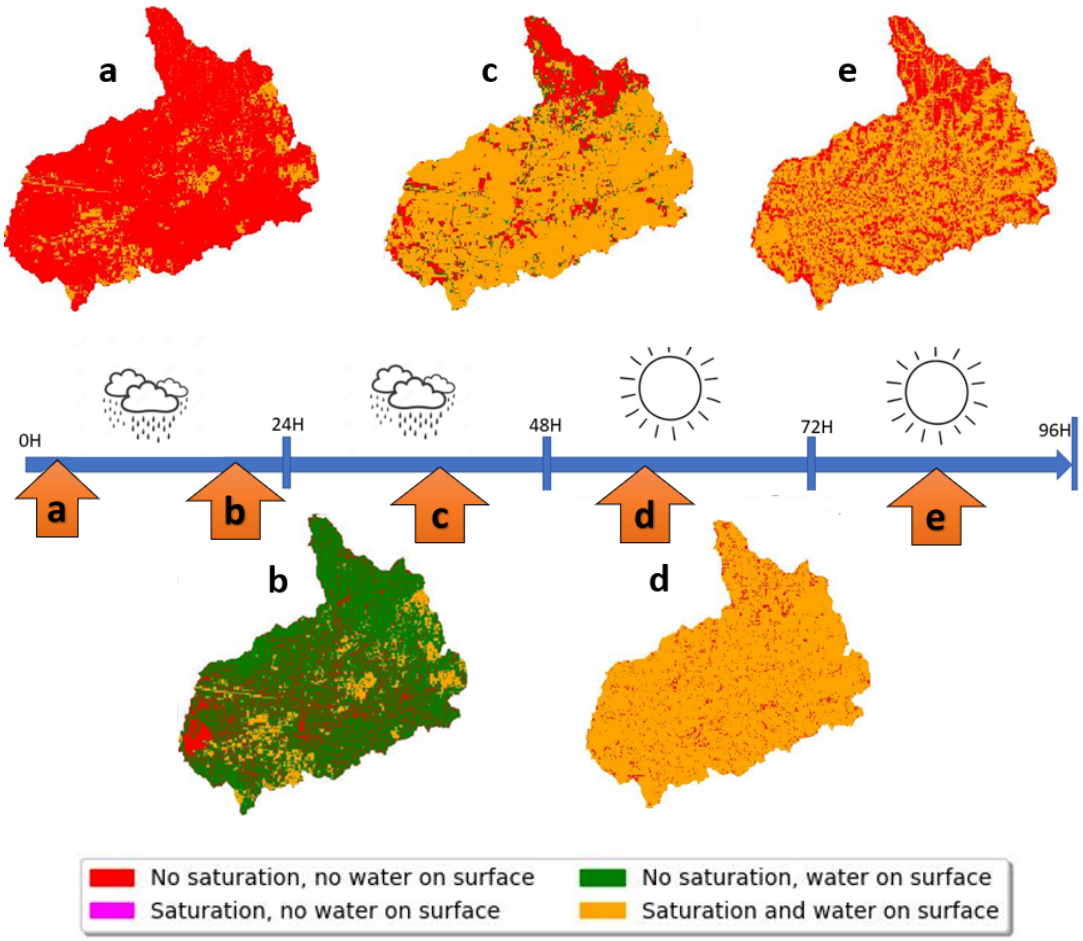

FIG. 6: Map of the states of the cells, at consecutive stages of the simulation. (a) The urbanized areas saturate first. (b) The surface water detention parameter traps some water at the surface, as it should. (c) The surface water has infiltrated the soil. The forests are not yet saturated. (d) The rain has stopped. The entire map has its soil saturated. Evaporation proceeds to dry the land. (e) End of the simulation. Evaporation has dried the surface to a large extent.

evaporation and thus flooding could potentially lie at higher risk. To observe this in the model, implementation of varying temperatures would be more realistic.

As mentioned in the results section, precipitation of 8 $mm.h^{-1}$ over 48 hours was implemented to observe the evolution of water runoff of the given region. For context, the region received an annual 500-600 mm rain in 2020 [18]. The world record for hourly rainfall is 305 mm (in Missouri, US) [19]. Future work on this aspect could be to compare real outcomes of water runoff against simulations of predicted weather conditions to see how similar the result are to actual reality.

The surface water detention was set to a constant; a third of the infiltration capacity of the corresponding land use. In their paper, Kassogué et. all [15] state having derived this parameter from high resolution satellite images. Such task could not have been performed within the frame of our study.

VII. CONCLUSIONS

Plotting the distribution of the total surface water quantified (see Figs. 5a and 5c) provides answers to our objectives. Our cellular automaton model clearly forms rivers corresponding to the ones actually observed in the studied region. Hence, the figures, along with the proof that water flows downstream too, provide evidence that the model can capture the water flow dynamics. Comparing Figs. 5b and Fig. 5d, we see that changing the land use, and covering the forest and agriculture areas with concrete and asphalt, will make the area more prone to flooding. For areas like the specific one studied here, consisting of an interplay between forest reserves, agricultural land, and infrastructure, this could lead to complications that should not be ignored in land-use policy-making.

There is room for future work such as improvement of precision for parameters related to soil type, varying

temperature, weather conditions to test how realistic water runoff of the model actually is. With improvements like these, this model could be potentially useful for water management and water flow analysis for any region in the world.

CONTRIBUTIONS

All participants collaborated on each part of the project, and contributed with an equal amount of work.

ACKNOWLEDGMENTS

We are grateful for the support of our tutor, Martin Selin, Turtle Alum, Filip Lindell, and our review group, the Ants. Great thanks also to Hamidou Kassogué, Mina Amharref, Abdessamed Bernoussi, Mustapha Maâtouk, Mustapha Ouardouz, whose research inspired our work.

[1] S. I. Seneviratne, X. Zhang, M. Adnan, W. Badi, C. Dereczynski, A. Di Luca, S. M. Vicente-Serrano, M. Wehner, and B. Zhou, 11 chapter 11: Weather and climate extreme events in a changing climate, (2021).

[2] M. G. Donat, A. L. Lowry, L. V. Alexander, P. A. O'Gorman, and N. Maher, More extreme precipitation in the world's dry and wet regions, Nature Climate Change **6**, 508 (2016).

[3] B. Clarke, F. Otto, R. Stuart-Smith, and L. Harrington, Extreme weather impacts of climate change: an attribution perspective, Environmental Research: Climate **1**, 012001 (2022).

[4] A. Sharma, C. Wasko, and D. P. Lettenmaier, If precipitation extremes are increasing, why aren't floods?, Water resources research **54**, 8545 (2018).

[5] G. J. Van Oldenborgh, K. Van Der Wiel, A. Sebastian, R. Singh, J. Arrighi, F. Otto, K. Haustein, S. Li, G. Vecchi, and H. Cullen, Attribution of extreme rainfall from hurricane harvey, august 2017, Environmental Research Letters **12**, 124009 (2017).

[6] B. Teufel, L. Sushama, O. Huziy, G. Diro, D. Jeong, K. Winger, C. Garnaud, R. De Elia, F. Zwiers, H. Matthews, *et al.*, Investigation of the mechanisms leading to the 2017 montreal flood, Climate Dynamics **52**, 4193 (2019).

[7] D. Loudyi, M. D. Hasnaoui, and A. Fekri, Flood risk management practices in morocco: facts and challenges, Wadi Flash Floods , 35 (2022).

[8] H. Kassogué, A. Bernoussi, M. Maâtouk, and M. Amharref, A two scale cellular automaton for flow dynamics modeling (2cafdym), Applied Mathematical Modelling **43**, 61 (2017).

[9] M. T. Anees, K. Abdullah, M. Nawawi, N. N. N. Ab Rahman, A. R. M. Piah, N. A. Zakaria, M. Syakir, and A. M. Omar, Numerical modeling techniques for flood analysis, Journal of African earth sciences **124**, 479 (2016).

[10] P. Horton, B. Schaefli, and M. Kauzlaric, Why do we have so many different hydrological models? a review based on the case of switzerland, Wiley Interdisciplinary Reviews: Water **9**, 3 (2022).

[11] E. Hasan and M. Elshamy, Application of hydrological models for climate sensitivity estimation of the atbara sub-basin, in *Nile River Basin* (Springer, 2011) p. 227.

[12] L. de Sousa, F. Nery, R. Sousa, and J. Matos, Assessing the accuracy of hexagonal versus square tilled grids in preserving dem surface flow directions, in *Proceedings of the 7th International Symposium on Spatial Accuracy Assessment in Natural Resources and Environmental Sciences (Accuracy 2006)* (Instituto Geográphico Português Lisbon, 2006) pp. 191–200.

[13] J. Kari, Cellular automata, University of Turku (2013).

[14] *Fact sheet 3 — Water in the atmosphere*, National Meteorological Library and Archive (2012).

[15] H. Kassogué, A. S. Bernoussi, M. Amharref, and M. Ouardouz, Cellular automata approach for modelling climate change impact on water resources, International Journal of Parallel, Emergent and Distributed Systems **34**, 21 (2019).

[16] C. Liao, T. Zhou, D. Xu, R. Barnes, G. Bisht, H.-Y. Li, Z. Tan, T. Tesfa, Z. Duan, D. Engwirda, *et al.*, Advances in hexagon mesh-based flow direction modeling, Advances in Water Resources **160**, 104099 (2022).

[17] A. Argun, A. Callegari, and G. Volpe, *Simulation of Complex Systems*, 2053-2563 (IOP Publishing, 2021).

[18] M. Meteo, 2020 annual climate report for morocco - maroc météo (2021), https://public.wmo.int/en/media/news-from-members/2020-annual-climate-report-morocco-maroc-meteo.

[19] W.M.O., World weather and climate extremes archive: Greatest sixty-minute (one hour) rainfall, https://wmo.asu.edu/content/world-greatest-sixty-minute-one-hour-rainfall.